

## Dipalmitoylphosphatidylcholine membranes modified with zeaxanthin: numeric study of membrane organisation

Witold Okulski <sup>a</sup>, Agnieszka Sujak <sup>b</sup>, Wiesław I. Gruszecki <sup>b,\*</sup>

<sup>a</sup> *Department of Biophysics, Medical Academy, Al. Racławickie 1, 20-059 Lublin, Poland*

<sup>b</sup> *Department of Biophysics, Institute of Physics, Maria Curie-Skłodowska University, 20-031 Lublin, Poland*

Received 11 April 2000; received in revised form 11 July 2000; accepted 26 July 2000

### Abstract

The model of a dipalmitoylphosphatidylcholine (DPPC) bilayer containing a xanthophyll pigment zeaxanthin (ZEA) is proposed. The model is based on the ten-state Pink-Green-Chapman model of a lipid monolayer. The Monte Carlo method of computer simulation has been applied. Our model of the lipid membrane consists of two lipid monolayers with ZEA molecules spanning the lipid bilayer. The concentration of ZEA molecules is assumed to be conserved. Within the model, the interactions between lipid monolayers in a bilayer exist through ZEA molecules only. The experimental data concerning the aggregation of ZEA in DPPC from the literature and from our research were applied as a criterion to fit the model parameters. The model gives the dependences of the main phase transition temperature on ZEA/DPPC molar ratio, the percentage of ZEA in a monomeric form on ZEA/DPPC molar ratio and on temperature. The dependences obtained within the model and the experimental ones are in qualitative agreement. The influence of intermolecular interaction parameters on ZEA aggregation has been discussed. The differences between the model and the experimental results concerning mainly the pattern of ZEA aggregation have been discussed. Analyses of the lipid microconfiguration allow to advance the hypothesis concerning the influence of ZEA on the membrane permeability. © 2000 Elsevier Science B.V. All rights reserved.

**Keywords:** Carotenoid; Xanthophyll pigment; Lipid membrane; Monte Carlo simulation; Molecular aggregate

### 1. Introduction

Carotenoid pigments play important physiological roles, mainly in photosynthesis [1] and as antioxidants [2]. The results of the research carried out in the last decade show, in addition, that carotenoid pigments and in particular polar carotenoids, xanthophylls, are important biomolecules modifying

the structural and dynamic properties of lipid membranes (see [3] for a review). Several experimental techniques have been applied to study the effect of carotenoid pigments on lipid membranes such as electron spin resonance [4–8], nuclear magnetic resonance [9,10], differential scanning calorimetry [11,12], circular dichroism [13], ultrasound absorption [14–16], quasi-elastic light scattering [17,18], fluorescence labelling of a lipid phase [19] and the interior of carotenoid pigmented liposomes [20]. In general, carotenoid pigments modify lipid membranes in a fashion similar to cholesterol, except the effect of xanthophylls is approximately twice as strong as this one observed in the case of cholesterol. Xanthophyll pig-

Abbreviations: ZEA, zeaxanthin; DPPC, dipalmitoylphosphatidylcholine; DMPC, dimyristoylphosphatidylcholine; MCS, Monte Carlo simulation; MCS/S, Monte Carlo step per site

\* Corresponding author. Fax: +48 (81) 5376191;  
E-mail: wieslaw.gruszecki@umcs.lublin.pl

ments in a concentration ranging from 1 to 10 mol% with respect to lipids generally rigidify the lipid phase in its fluid state but do not have a pronounced effect or slightly fluidise the ordered lipid phases [3]. Carotenoid pigments present in the lipid membranes also generally decrease the cooperativity of the phase transition [3]. Such effects are rather typical for several lipid membrane modifiers. The interaction of foreign molecules with lipid membranes has been the topic of many theoretical studies. The Monte Carlo simulation (MCS) method has been widely used for studying these systems [21–28]. In most of the reported applications of the MCS method, the models of lipid bilayer or monolayer with the parameters describing intermolecular interactions are proposed and the dependences generated by MCS are compared with the experiments to test the initial hypotheses. The MCS is carried out on a triangular lattice [28]. Each acyl chain of a lipid molecule is assigned to a site in the lattice to account for the extended volume effect, i.e. two chains cannot occupy the same lattice site (volume) simultaneously. Foreign molecules may be distributed as large molecules (peptides or proteins) occupying several lattice sites or as small molecules (cholesterol, anaesthetics). The latter molecules can be treated in two ways [27]: (a) as substitutional impurities taking the place of lipid chain, i.e. occupying one lattice site like cholesterol [21]; (b) as interstitial impurities which can be distributed between lipid chains (like some anaesthetics [27]) without any change of a membrane surface. The way foreign molecules should be treated is not precisely dependent on their molecular size but rather on their amphipathic nature and interactions with lipid molecules, as concluded by Jørgensen et al. [27].

Zeaxanthin (ZEA), the polar carotenoid pigment on which we focus our attention in the present work, is regarded as an interstitial impurity. There are two main reasons to justify such an assumption. The first reason is the relatively good solubility of ZEA in the lipid phase [3], which is indicative of small entropy of mixing. In such a case the non-substitutional or interstitial treating is preferred. Moreover, a description based on the canonical ensemble should be used [27] under the natural assumption that the number of ZEA molecules within the membrane is conserved. The second reason is that the total enthalpy change (i.e. the sum of the enthalpies of the pretransition

and the main phase transition) of ZEA-dipalmitoylphosphatidylcholine (DPPC) vesicle suspension remains close to the value obtained for the DPPC alone [12]. It means that the enthalpy change is nearly independent of ZEA concentration, like for interstitial impurity [27].

Although the general picture of the organisation of xanthophyll-lipid membranes seems to be well understood [3], the microscopic model of a lipid membrane with ZEA has not been analysed yet. The aim of this paper is to present the theoretical model of the DPPC membrane modified with ZEA that is consistent with the basic experimental results concerning this system, such as the main phase transition temperature and the temperature dependence of the percentage of ZEA in monomeric and aggregated forms. Aggregation of xanthophyll pigments in lipid membranes is one of the main phenomena responsible for organisation of this system and seems to play an important role in the action of carotenoids in membranes [3]. The process of aggregation of ZEA in the DPPC membranes was a subject of our experimental investigation [29]. In the next sections we present the theoretical model of the DPPC bilayer containing ZEA followed by the results of the calculations performed and the discussion.

## 2. The model of lipid membrane and calculation methods

The numerical calculations presented below are based on the ten-state Pink-Green-Chapman model [26,28,30]. The model of the lipid membrane consists of two lipid monolayers with ZEA molecules which have the same position in both monolayers as rigid rods, always set up perpendicularly to the membrane surface with each polar end placed in the lipid monolayer (Figs. 1 and 2). The concentration of ZEA molecules is assumed to be conserved. Within the model, the interactions between lipid monolayers in a bilayer exist through ZEA molecules only. A two-dimensional triangular lattice represents each monolayer. Each site of the lattice is occupied by an acyl chain of a lipid molecule. ZEA molecules are placed in the interstitial points (Fig. 1).

Each lipid chain can exist in one of ten states: the all-*trans* ground state (the first state); eight inter-

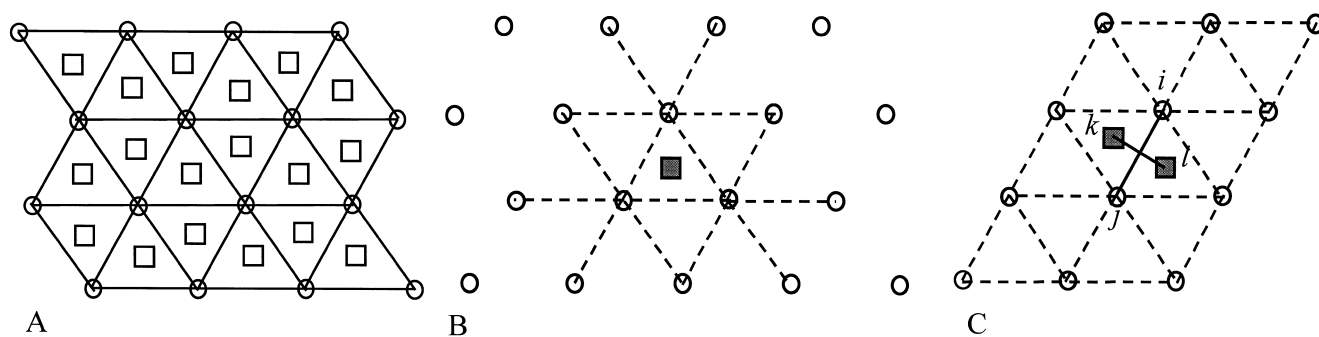


Fig. 1. Lattice model of the lipid monolayer. (A) The sites indicated by circles are occupied by lipid chains; the sites which can be occupied by ZEA molecules are indicated by squares. (B) Lipid-lipid interactions weakened by a ZEA molecule (black square) are marked by broken lines. (C) Only the stronger of two the interactions between  $i$  and  $j$  lipid chains or  $k$  and  $l$  ZEA molecules contributes to the Hamiltonian.

mediate states (2, ..., 9), which are low energy excitations of the all-*trans* state; the tenth high energy 'melted' state which is a component of the high temperature fluid phase. States 2–9 are characteristic of the high temperature gel phase. All states of chain  $\alpha$  are described by the conformational energy  $E_\alpha$ , area  $A_\alpha$  and degeneracy  $D_\alpha$  [28]. The ZEA molecule is characterised by  $A_Z = 30.0 \times 10^{-20} \text{ m}^2$ ,  $E_Z = 0$  and  $D_Z = 1$ .

The model Hamiltonian of each of the two lipid monolayers consists of four components:

$$H = H_1 + H_2 + H_3 + H_4 \quad (1)$$

The first one is a single-chain contribution:

$$H_1 = \sum_{i=1}^N \sum_{\alpha=1}^{10} E_\alpha L_{\alpha i} \quad (2)$$

where  $N$  is the number of chains in a monolayer and  $L_{\alpha i} = 1$ , when chain  $i$  is in state  $\alpha$ , otherwise  $L_{\alpha i} = 0$ . The second contribution,  $H_2$ , describes the interaction between lipid chains:

$$H_2 = -\frac{J_0}{2} \sum_{i,j=1\alpha}^N \sum_{\beta=1}^{10} w_{ij}^{LL} V_\alpha V_\beta S_\alpha S_\beta L_{i\alpha} L_{j\beta} \quad (3)$$

Here,  $J_0$  is the interaction strength between two nearest neighbour all-*trans* chains,  $V_\gamma = (A_1/A_\gamma)^{-5/4}$ ,  $\gamma$  denotes the number of the lipid chain state in the range 1–10. The order parameter of the acyl chain in the  $\gamma$  state ( $S_\gamma$ ) can be written in the form [28]:  $S_\gamma = 1.8A_1A_\gamma^{-1} - 0.8$  for the geometrical reason. For  $\alpha = 10$ , a 'weakening factor' is used, therefore  $V_{10}$  is

replaced by  $0.4V_{10}$  [28]. The summation in Eq. 3 is over the nearest neighbours only. The weakening factor,  $w_{ij}^{LL}$ , is used to introduce the attenuation of lipid-lipid interactions by ZEA molecules.

(i)  $w_{ij}^{LL} = 0.65$  for sites  $i$  and  $j$  in the neighbourhood of ZEA (Fig. 1B) provided that the lipid chains at sites  $i$  and  $j$  are not in the tenth melted state. This value of factor  $w_{ij}^{LL}$  was adjusted to obtain the temperature of the main phase transition ( $T_m$ ) close to  $41^\circ\text{C}$  for 5 mol% of ZEA [12]. It appeared that it was not simple to match  $w_{ij}^{LL}$  to  $T_m$  and to correct the percentage of the ZEA molecules in molecular aggregates. The smaller value of this factor causes that the

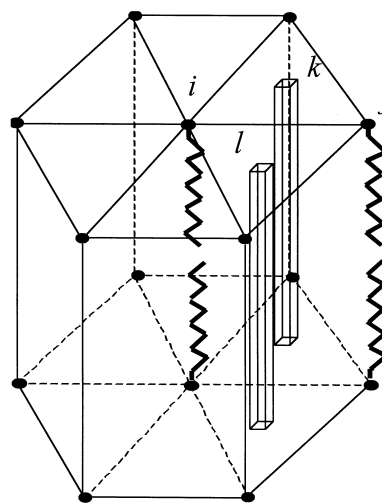


Fig. 2. Lattice model of the lipid bilayer containing ZEA molecules (represented by bars). The attraction of ZEA molecules at sites  $k$  and  $l$  may be weakened by states of the four nearest neighbouring lipid chains at sites  $i$  and  $j$ .

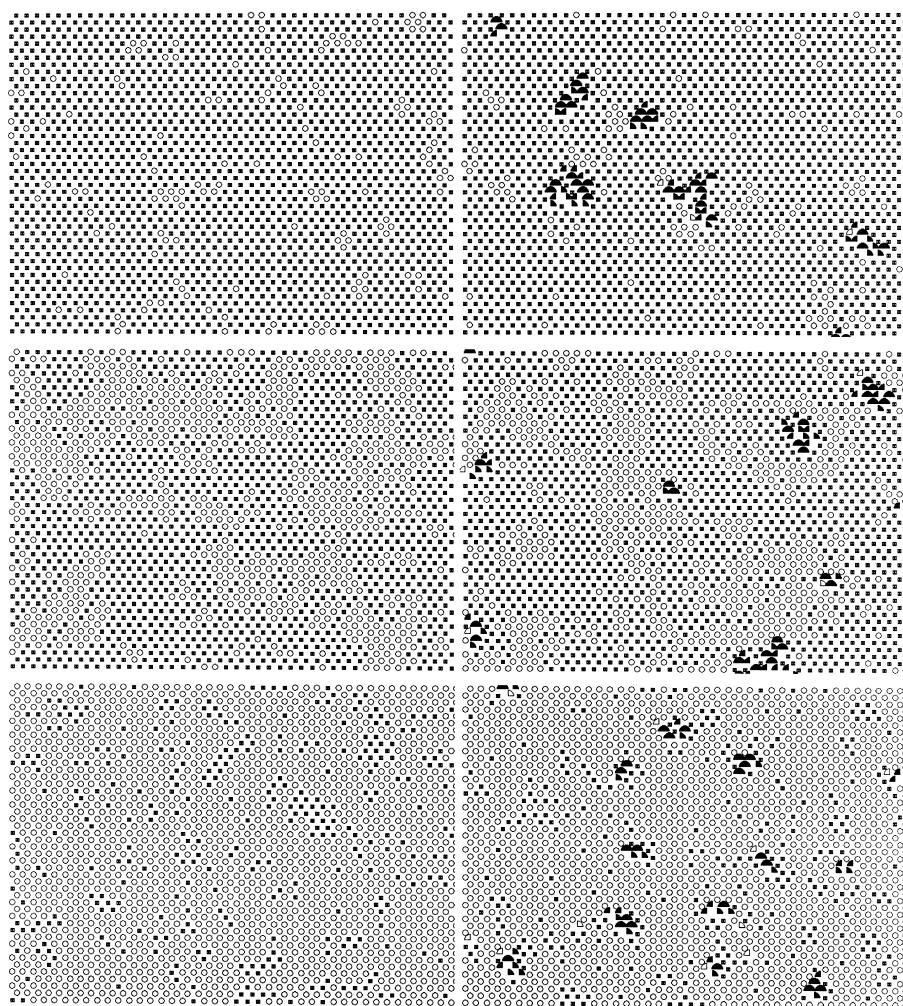


Fig. 3. Snapshots of microconfigurations of DPPC-ZEA bilayer (a fragment of one of two monolayers is shown). There are ZEA molecules distributed at interstitial positions near pie slices. Empty circles and empty pie slices denote positions of acyl chains in the fluid state, filled squares and filled pie slices donate the gel state. On the left, pure DPPC; on the right, DPPC+5 mol% ZEA. Upper row:  $T=35^{\circ}\text{C}$  (below the phase transition); middle row:  $T=41^{\circ}\text{C}$  for DPPC and DPPC+5 mol% ZEA (at the phase transition); bottom row:  $T=47^{\circ}\text{C}$  (above the phase transition).

absolute value of ZEA binding energy increases, as compared to the energy of the surrounding lipid chains. Moreover, the lower value of  $w_{ij}^{\text{LL}}$  causes that ZEA molecules tend to be placed more closely in relation to each other to decrease the area of weakened lipid chain attraction, therefore the tendency of ZEA to aggregation is stronger.

(ii)  $w_{ij}^{\text{LL}} = 0$  provided that the line connecting sites  $i$  and  $j$  is perpendicular to the line crossing the sites  $k$  and  $l$  of the two nearest neighbour ZEA molecules (Fig. 1c) and interaction of ZEA molecules is stronger than the one of  $i$  and  $j$  lipid chains, i.e.  $0.65V_{\alpha}V_{\beta}S_{\alpha}S_{\beta} < I_{\text{ZZ}}w_{\text{kl}}^{\text{ZZ}}$ ;  $\alpha$  and  $\beta$  denote the states

of  $i$  and  $j$  lipid chains,  $w_{\text{kl}}^{\text{ZZ}}$  and  $I_{\text{ZZ}}$  are defined below, following Eq. 5.

(iii)  $w_{ij}^{\text{LL}} = 1$  in other cases.

Condition (ii) describes the behaviour of neighbouring ZEA and lipid molecules: if the attraction of the neighbouring ZEA molecules is stronger than the attraction of the neighbouring lipid chains the pigment molecules are approaching one another and the lipid molecules are receding. In accordance with this, only the stronger of the two interactions (the  $i$  and  $j$  lipid chains or  $k$  and  $l$  ZEA molecules) contributes to the Hamiltonian.

The third contribution of the Hamiltonian,  $H_3$ , is

the energy of the interaction between polar parts of molecules:

$$H_3 = \Pi \sum_{i=1}^N \sum_{\alpha=1}^{10} A_{\alpha} L_{\alpha i} + \Pi \sum_{k=1}^M A_Z L_{Zk} \quad (4)$$

where  $\Pi$  is the intrinsic lateral pressure.

Contribution  $H_4$  accounts for the lipid-ZEA and ZEA-ZEA interactions:

$$H_4 = -J_0 \sum_{k=1}^M \sum_{h(k)=1}^3 \sum_{\alpha=1}^{10} V_{\alpha} S_{\alpha} L_{\alpha h(k)} L_{Zk} - \frac{J_0}{2} \sum_{k,l}^M I_{ZZ} w_{kl}^{ZZ} L_{Zk} L_{Zl} \quad (5)$$

The numbers  $k$  and  $l$  denote interstitial sites accessible for ZEA and the numbers  $i$  and  $j$  the lipid chain lattice sites. The summations are always over neighbouring sites only. The second component of  $H_3$  is constant for the constant ZEA/DPPC molar ratio assumed in our calculations. Because the main results of the simulation depend on changes in energy, this component could be neglected. According to the model, a ZEA molecule interacts with three neighbouring lipid chains and may interact with three ZEA molecules, placed at the interstitial sites of neighbouring triangles. The second sum of Eq. 5 runs over the three lipid sites  $h(k)$ , neighbouring the ZEA site  $k$ .

The weakening factor  $w_{kl}^{ZZ}$  depends on a state of two lipid chains at sites  $i$  and  $j$  within each of the two monolayers (as depicted in Fig. 2):

$$w_{kl}^{ZZ} = (V_{\alpha} S_{\alpha} V_{\beta} S_{\beta} V_{\delta} S_{\delta} V_{\gamma} S_{\gamma})^q \quad (6)$$

under the condition that  $w_{ij}^{LL} = 0$ .  $\alpha, \beta, \delta, \gamma$  denote the states of the lipid chains at sites  $i$  and  $j$ . Otherwise  $w_{kl}^{ZZ} = 0$ . The parameter  $I_{ZZ}$  has been fixed as 1.02 and the value of  $q$  as 1.

In the model, the translational lipid degrees of freedom are neglected. The lateral movements of ZEA molecules are permitted and are performed every five Monte Carlo steps per site (MCS/S). The rules of the movement of ZEA molecules are as follows:

1. All possible ZEA dislocations are considered

while finding a ZEA molecule in a succeeding Monte Carlo step.

2. The states of two lipid chains (one in each monolayer) which will interact with the ZEA molecule after its dislocation but did not interact before, are randomly selected.
3. For each dislocation, the change of the microstate free energy  $\Delta E$  is calculated.
4. A displacement is accepted for the lowest  $E$  under the condition that  $\exp(-\Delta E/k_B T) > \xi$ , where  $\xi \in [0,1]$  is a random number,  $k_B$  denotes the Boltzmann constant and  $T$  is the temperature.

The computer simulation was performed for the system containing 10 000 sites (lipid chain sites) in each of the two lattices i.e. 10 000 molecules of DPPC placed in two monolayers. A certain number of mol% of ZEA was added. The periodic boundary conditions are assumed. In the model  $\Pi = 0.030$  N/m and  $J_0 = 0.70985 \times 10^{-20}$  J [28]. These values give an expected temperature of 41.2°C of the main phase transition of the pure DPPC bilayer.

ZEA molecules are distributed randomly in the lattice of lipids, which has been equilibrated earlier by 1000 MCS/S. Several thousand MCS/S were carried out in order to obtain the thermodynamic equilibrium.

### 3. Results of calculations and discussion

#### 3.1. Membrane organisation and the main phase transition temperature in the presence of ZEA

The snapshots of the DPPC-ZEA monolayer microconfiguration (Fig. 3) demonstrate a cluster structure of the lipid membrane, evident especially at temperatures close to the main phase transition ( $T_m$ ). The cluster is defined here as a microdomain containing at least seven neighbouring acyl chains in a non-dominant state. For instance, below the  $T_m$  the cluster is composed of a group of at least seven acyl chains in the fluid state, embedded in the gel bulk phase. The aggregates of ZEA are also seen in Fig. 3. There are very few ZEA monomers which can be noticed. The reason is that neighbouring ZEA molecules may be qualified as monomers if their attrac-

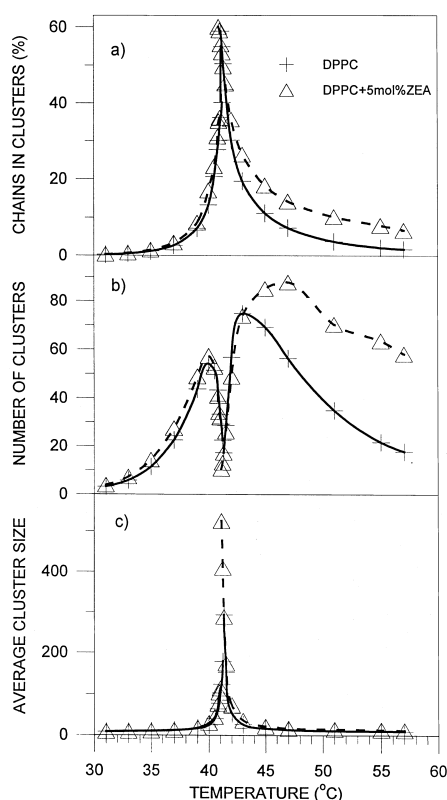


Fig. 4. Computer simulation data. Temperature dependences of (a) percentage of acyl chains in clusters, (b) number of clusters, and (c) average cluster size for the pure DPPC and the DPPC+5 mol% ZEA membrane.

tion is weaker than the attraction of the closest acyl chains (see point (ii) in Section 2).

The results presented in the figures below are averaged over the two monolayers of a lipid bilayer and refer to one monolayer.

Fig. 4a presents the temperature dependence of a percentage of lipid chains in the cluster structures. As can be seen, the presence of ZEA results in an increase in the number of lipid chains in the gel clusters, above the  $T_m$ . Figs. 3 and 4b indicate that the effect of ZEA in the increase in the number of the gel clusters is significant above the  $T_m$ . A slightly greater number of lipid chains may be found in the fluid clusters, below the  $T_m$  (Fig. 4b). ZEA molecules induce formation of gel clusters within their surroundings in the fluid phase (above the  $T_m$ ) (Fig. 3). The average cluster size, defined as the ratio of the number of chains in clusters and the number of clusters, remains nearly the same in both ZEA containing and pure DPPC membranes (Fig. 4c). An exception is the

phase transition region in which the average size of clusters is evidently greater owing to the presence of ZEA (Figs. 3 and 4c). As can be seen (Fig. 4b), a sharp decrease in the number of clusters was observed directly in the temperature region of the  $T_m$ . This is an indication that the conversion of the non-dominant phase (the clusters) into the bulk dominant phase goes via the association of small clusters into the greater ones.

Another parameter to be compared in the pure DPPC and ZEA containing lipid membranes is an order parameter. The average acyl chain order parameter is calculated as:

$$S_{av} = \frac{1}{N} \sum_{i=1}^N \sum_{\alpha=1}^{10} S_{\alpha} L_{\alpha i} \quad (7)$$

The temperature dependences of  $S_{av}$  for pure DPPC and DPPC+5 mol% ZEA are shown in Fig. 5. The values of  $S_{av}$  below the  $T_m$  are slightly lower owing to the ZEA presence in the membrane. The rapid decrease in  $S_{av}$  above the phase transition temperature is not as sharp in the presence of ZEA, which is an indication of the decreased cooperativity of the transition. The most pronounced effect of ZEA on the order parameter is visible in the fluid phase of DPPC, above the main phase transition. The addi-

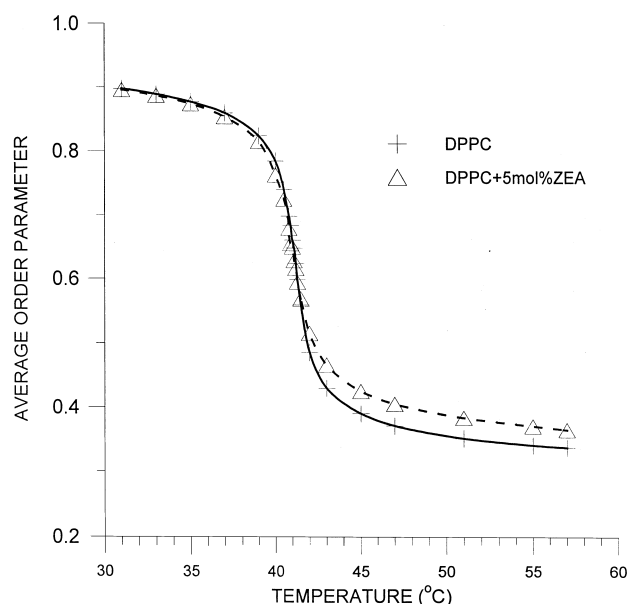


Fig. 5. Average order parameter of an acyl chain as a function of temperature. Computer simulation data.

tion of 5 mol% ZEA to the membrane results in the increase of the average order parameter in this phase. This fact suggests that despite the fact that ZEA weakens slightly the lipid interactions within the pigment surroundings (see Eq. 3 and Fig. 1B) the ZEA affinity to acyl chains in the gel state is dominant and ZEA molecules constrain the gel state within their neighbourhood. This effect is particularly pronounced above the  $T_m$ . In summary, the analysis of the average order parameter shows that ZEA makes the membrane slightly more fluid below the  $T_m$  and clearly more ordered above the  $T_m$ . Such an effect of polar xanthophylls with respect to lipid membranes was observed in most experiments carried out with the application of different techniques [3].

The midpoint temperature in a dependence  $S_{av}(T)$  can be interpreted as corresponding to the main phase transition,  $T_m$ . The values of  $T_m$  for DPPC membranes modified with ZEA are listed in Table 1.

Another parameter to be analysed is specific heat. Specific heat of the membrane,  $C(T)$ , in accordance with the fluctuation-dissipation theorem, can be written as:

$$C(T) = \frac{1}{k_B T^2} [(H^2)_{av} - (H_{av})^2] \quad (8)$$

The averages in Eq. 8 have been calculated over several hundred membrane microstates, taken every ten

MCS/S after the appropriate number of MCS/S (up to 30 000 near the  $T_m$ ) following the change of temperature.

Fig. 6 presents, calculated numerically, the temperature dependences of specific heat per lipid molecule  $C(T)$  for the DPPC membranes containing different molar fractions of ZEA. As can be seen clearly, the dependence has a peak position corresponding to the phase transition temperature  $T_m$ . The values of the  $T_m$  found from the peak positions are listed in Table 1.

The maximum in the  $C(T)$  dependence obtained from our simulations does not need to point exactly at the  $T_m$  and the method of Ferrenberg and Swendsen [31] should rather be used. This method has not been applied in the present study because our main aim has been to show the qualitative rather than quantitative changes of thermal dependences due to the ZEA presence in the lipid membrane.

As can be seen from Fig. 6 and Table 1 the increase in a molar fraction of ZEA in DPPC results in a decrease in the  $T_m$  calculated, based on the computer simulation. The same effect of a decrease in the value of  $T_m$ , corresponding to an increase in the ZEA concentration, can also be observed in the calorimetric experiments [12], in the pigment concentration range between 0 and 3 mol%.

As is shown in Fig. 6, the half-height width of the transition increases upon increasing the molar ratio

Table 1

The main phase transition temperature  $T_m$  of the DPPC membranes containing ZEA in different concentration as found from different parameters

Molar ratio of ZEA/DPPC (mol%)	Main phase transition temperature (°C)		
	Peak position of specific heat – computer simulation <sup>a</sup>	Order parameter – computer simulation <sup>b,c</sup>	Peak position of specific heat – experiment – read from Fig. 3 in [12]
0	41.2	41.20	41.4
1	41.0	41.03	40.7
2	41.0	41.03	40.3
3			40.3
4	41.1	41.05	
5	41.0	41.04	
6			40.9

<sup>a</sup>Typical error  $\pm 0.1^\circ\text{C}$ .

<sup>b</sup>Typical error  $\pm 0.05^\circ\text{C}$ .

<sup>c</sup>The values of  $T_m$  found from the average order parameter are read as a point of intersection of the curve in Fig. 5 and a horizontal line at the level of the average of order parameters for  $(41 \pm 16)^\circ\text{C}$ .

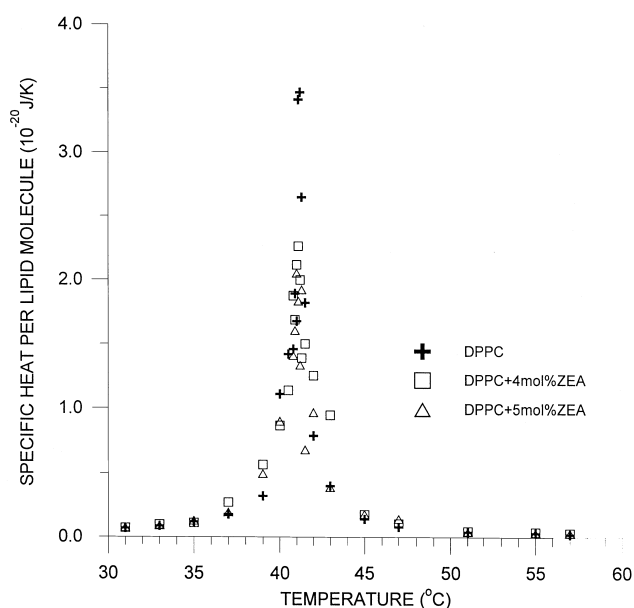


Fig. 6. Computer simulation data. Temperature dependence of specific heat per lipid molecule. Results for different ZEA/DPPC molar ratios are shown as indicated.

of ZEA. The broadening of  $C(T)$  peaks is indicative of the decreased cooperativity between the lipid molecules, related directly to the presence of ZEA.

According to the model, the value of the  $T_m$  should decrease upon decreasing the absolute value of the lipid-lipid attraction energy. For instance, the  $T_m$  of the dimyristoylphosphatidylcholine (DMPC) membrane has a lower value than the one of the DPPC membrane, because of the differences in the length of alkyl chains [32]. A ZEA molecule weakens the acyl chain-acyl chain interaction within its neighbourhood (cf. Fig. 1B). As can be concluded from the model, the number of weakened bonds per single ZEA molecule is greatest in the case of the monomeric form of the pigment. Therefore, the greater the number of ZEA monomers, the smaller the value of the  $T_m$  may be expected. Fig. 7a presents the temperature dependences of the number of ZEA monomers calculated following the numerical simulation according to our model. As can be seen, the number of ZEA molecules in the monomeric state increases upon the increase of the ZEA/DPPC molar ratio. This seems to be one of the main reasons for the ZEA related decrease in the temperature of the main phase transition.

### 3.2. Zeaxanthin aggregation in the lipid membrane

Fig. 7 presents numerically simulated temperature profiles of ZEA in the monomeric state in the membranes containing different molar fractions of the pigment. As can be seen, the percentage of ZEA monomers increases upon the increase in temperature. In particular, the concentration of ZEA monomers and  $N$ -aggregates was found to depend on a pigment concentration above the  $T_m$  (Figs. 7b and 8). A similar effect was also observed in the experiment [29]. It is interesting that the percentage of the monomeric form of ZEA, far below the  $T_m$ , tends approximately to the same value of 20% for all examined ZEA/DPPC molar ratios upon decreasing the temperature. This effect was also observed in the experiment [29].

As can be seen (Fig. 9), an increase in temperature leads to a decrease in the percentage of ZEA in  $N$ -aggregated form ( $N > 4$ ). This effect can also be observed in the experimental dependence [29]. The per-

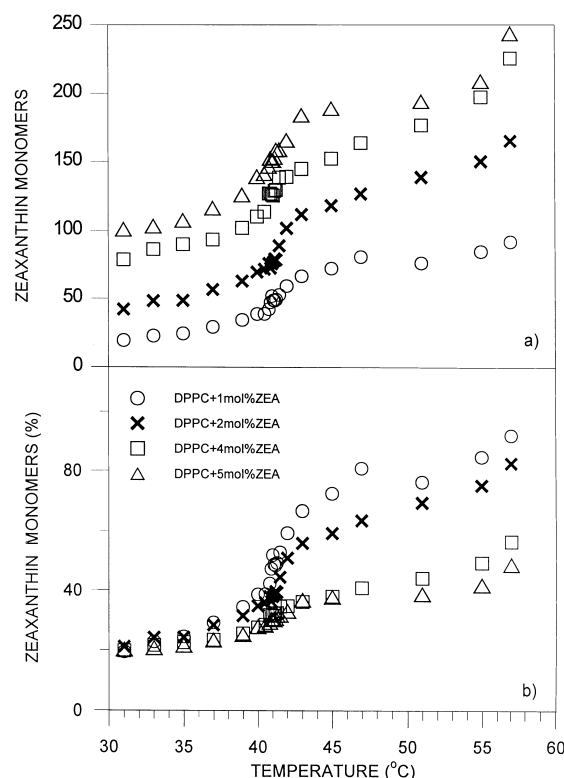


Fig. 7. Computer simulation data. (a) Number of ZEA monomers; (b) percentage of ZEA monomers as a function of temperature.



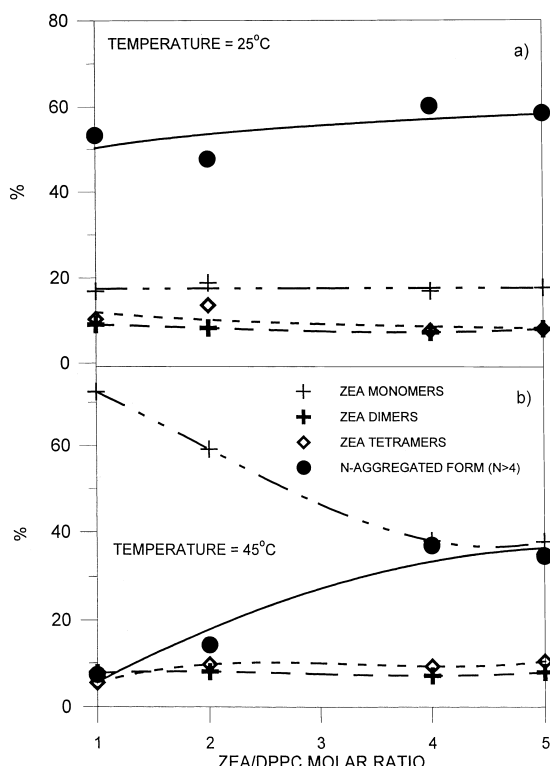


Fig. 8. Computer simulation data. Percentage of the monomeric and aggregated forms of ZEA at 25°C (below the phase transition) and 45°C (above the phase transition) as a function of ZEA/DPPC molar ratio.

centage of monomers calculated theoretically for 5 mol% ZEA increases from about 20% in 30°C to about 40% in 50°C. The percentage of the *N*-aggregated form decreases from 58% to 30% at the same temperatures. The experimental values are 37% and 58% as a percentage of the monomers and 8% and 4% as a percentage of the *N*-aggregated form correspondingly [29]. A significant qualitative difference between the experimental and the model values of the percentage of the *N*-aggregated form is observed. The reasons for such a difference are the following.

The analyses of the experimental results [29] indicate that the percentages of the dimers and the *N*-aggregates are approximately constant, except local extrema near the  $T_m$ . The dissociation of the tetrameric molecular forms seems to be the main reason for the monomerisation in the course of the membrane fluidisation. The hypothesis has been put forward [29] that the large molecular aggregates of ZEA are composed of dimers, in which the ZEA molecules are bound to one another more tightly, owing to the

hydrogen bonding between the hydroxyl groups located at the 3 and 3' positions of the carotenoid molecules, rather than the dimers in the aggregate.

The dependence of the ZEA aggregation level on pigment concentration within the lipid phase is more pronounced in the fluid state of the membrane than below the phase transition (Fig. 8). It is interesting that the fractions of ZEA molecules in the dimeric and tetrameric structures are almost independent of pigment concentration (that is also seen in the experimental dependences [29]). It means that the numbers of ZEA molecules in dimers and tetramers are proportional to the ZEA/DPPC molar ratio.

Several factors are able to influence the aggregation level of ZEA in the lipid phase of DPPC in our model. The factors in favour of the formation of molecular aggregates of ZEA are as follows:

1. The value of the parameter  $I_{ZZ}$  (Eq. 5). The higher the value of  $I_{ZZ}$ , the higher the energy of ZEA aggregation.
2. The value of the parameter  $w_{ij}^{LL}$ . The smaller attenuation area of the lipid-lipid interaction in the surroundings of the ZEA aggregate than in the surroundings of the separate monomers forming this aggregated structure. The smaller the value of  $w_{ij}^{LL}$  the stronger the attenuation.
3. The condition (Eqs. 3 and 5) according to which only one energy term, the energy of the stronger one out of the lipid-lipid or ZEA-ZEA interactions, contributes to the Hamiltonian. The latter interaction may be stronger within the attenuation area.
4. The tendency of ZEA molecules to be placed near acyl chains in the gel state: gel clusters promote formation of ZEA aggregates.

The factors that make ZEA aggregation less probable are as follows:

1. A smaller value of the parameter  $I_{ZZ}$  (Eq. 5).
2. Weaker attenuation of the lipid-lipid interaction within the surroundings of a ZEA molecule (a higher value of  $w_{ij}^{LL}$  but smaller than 1).
3. The diffusion of ZEA molecules to fluid areas within a membrane containing gel or fluid clusters, owing to the attenuation of the weaker lipid-lipid attraction in these areas. On the other hand, ZEA molecules attract stronger acyl chains

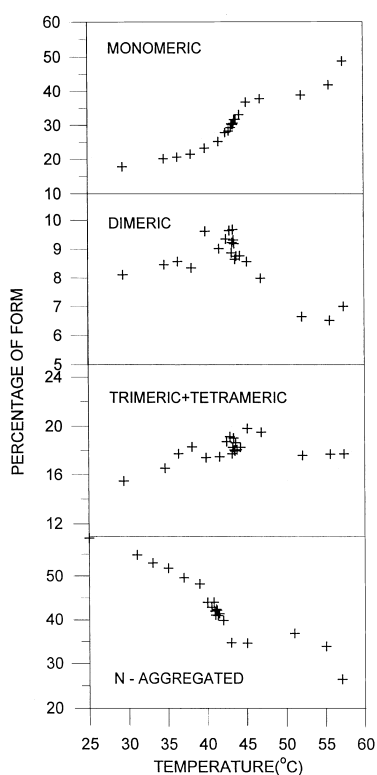


Fig. 9. Computer simulation data. Percentage of the monomeric and aggregated forms of ZEA in the DPPC+5 mol% ZEA membrane as a function of temperature.

in the gel state than in the fluid state. This means that pigment molecules tend to be localised within the interfacial region at the gel side.

4. Attenuation of the ZEA-ZEA attraction in fluid surroundings (Eq. 6).
5. Attenuation of the lipid-lipid interaction by ZEA, which causes that below the  $T_m$  ZEA molecules are surrounded by acyl chains in the fluid state. These chains, in turn, attenuate the ZEA-ZEA attraction interactions (Eq. 6).

### 3.3. Influence of ZEA on the membrane small ion permeability

Pure lipid membranes are almost impermeable to ions except the phase transition region, in which the permeability rapidly increases [33]. A number of theoretical papers have appeared to explain this phenomenon [21,28,34,35]. According to the current hypothesis, the enhancement of the passive ion permeability observed is related to the area of the interfacial regions, separating the clusters (non-dom-

inant phase) and the bulk dominant phase. The interfacial regions can contain structural defects because of a mismatch in molecular packing, which are directly related to the leakiness of a membrane.

According to our model, the interfacial region consists of fluid borders of gel areas and gel borders of fluid areas. The gel (fluid) area is defined as a group of at least seven acyl chains in the gel (fluid) state, which adjoin each other. This definition of the gel and fluid areas is similar to the definition of a cluster but does not require the condition concerning dominant and non-dominant phases. The border of a given area consists of those acyl chains that are nearest neighbours of the chains of this area.

As can be seen from Fig. 10, the size (area) of the interfacial region increases significantly owing to the presence of ZEA, except the temperature region close to and below the  $T_m$ , in which the effect is relatively weak. A detailed analysis of the computer snapshots of the molecule microconfigurations (Fig. 3) indicates that, especially above the  $T_m$ , there are some ZEA molecules which are the nearest neighbours of the lipid chains in the fluid phase. A mismatch of molecular packing within these contact areas may be expected. Comparing the area of the interfacial region shown in Fig. 10 and the area of the fluid borders of ZEA (Fig. 11) (in general these areas may

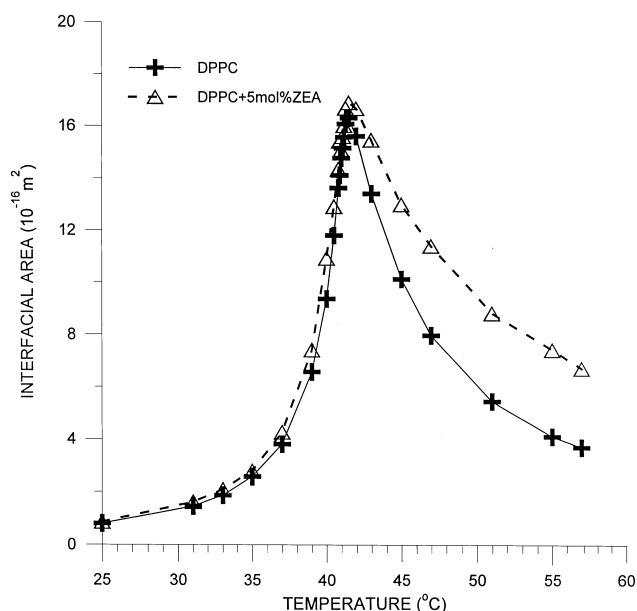


Fig. 10. Computer simulation data. Interfacial area as a function of temperature.

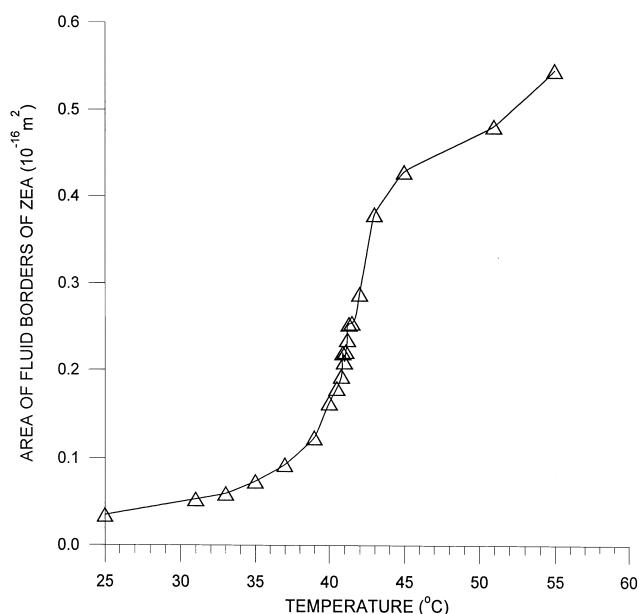


Fig. 11. Computer simulation data. Area of the fluid borders of ZEA molecules in the DPPC+5 mol% ZEA membrane as a function of temperature.

overlap), we conclude that fluid borders of ZEA molecules, for 5 mol% of ZEA, can increase the region of the enhanced permeability by less than about 4% at 25°C, 1% at the  $T_m$  and 8% at 55°C.

The interesting question that now arises is whether the interfacial region acts as a 'sink for impurities' in the case of the presence of ZEA in the membrane. Fig. 12 shows the temperature dependence of the percentage of ZEA molecules present in the interfacial area. In the model, each ZEA molecule is ascribed to the proximate acyl chain placed at the left-hand side (looking from the lipid head site). A ZEA molecule is recognised as placed in the interfacial area under the condition that the corresponding acyl chain is placed in this area. As can be seen from Fig. 12, the percentage of ZEA in the interfacial region increases upon the increase in temperature up to the  $T_m$ , for all ZEA molar ratios, and above the  $T_m$ , for 4 and 5 mol% ZEA only. This effect ranges from a few percent at 35°C up to 30–40% at 55°C. Only a few percent of ZEA molecules are distributed in the interfacial region far below the  $T_m$  because of the very small area of this region (Fig. 10). As can be seen from Fig. 12 the mechanism responsible for the distribution of ZEA molecules in the interfacial region is more complex. The snap-

shots of the microconfiguration indicate that there are acyl chains mainly in the gel state between aggregated ZEA molecules in the temperature region of the  $T_m \pm 15^\circ\text{C}$ . This observation can be interpreted as being directly related to the stronger attraction of ZEA molecules with acyl chains in the gel state than in the fluid state. This action of the ZEA aggregates to conserve the gel clusters above the  $T_m$  (Fig. 3) seems to be the reason for the increase in the size of the interfacial region (Fig. 10). The shapes of the small molecular aggregates of ZEA fit better the shapes of the interfacial regions above the  $T_m$  than the shapes of the large aggregates below the  $T_m$  (as can be seen from the snapshots of the microconfigurations). This mechanism is the reason why the percentage of ZEA in the interfacial region above the  $T_m$  is greater than the one just below the  $T_m$  for 4 and 5 mol% ZEA.

Fig. 12 shows that the lower the molar ratio of ZEA, the lower the percentage of ZEA in interfacial region far above the  $T_m$ . Simultaneously, there is a greater percentage of ZEA in the monomeric form corresponding to the lower molar ratio of ZEA (Fig. 7). Another open question is why the ZEA monomers are not situated within the interfacial region. In contrast to a ZEA aggregate, a ZEA monomer does

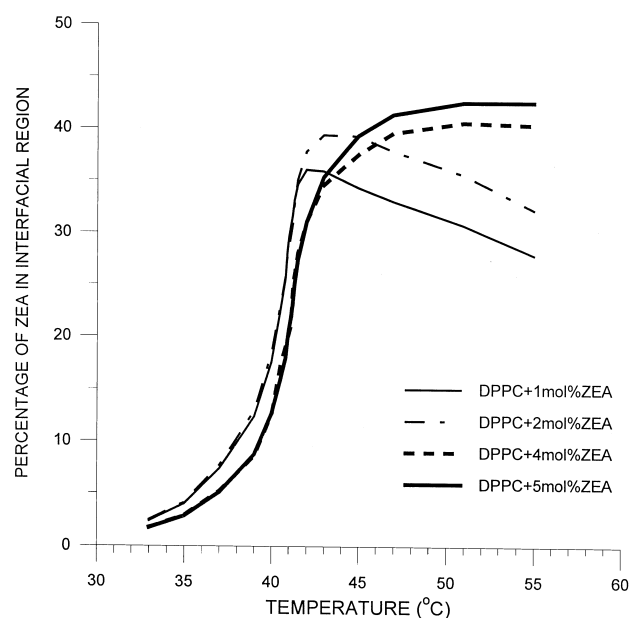


Fig. 12. Temperature dependence of percentage of ZEA molecules in the interfacial region for different ZEA/DPPC molar ratios as indicated. Computer simulation data.

not seem to be able to create and conserve a gel cluster above the  $T_m$ . Fig. 12 indicates that there are about 43% of ZEA molecules within the interfacial region at 5 mol% pigment concentration and about 28% at 1 mol% at 55°C. In the case of the low molar ratios of ZEA (1 and 2 mol%) the mechanism of vanishing of the interfacial regions dominates the effect of the shape fitting discussed above.

One can expect that ZEA will increase the membrane permeability, in particular at temperatures above the  $T_m$ , assuming that the permeability is directly related to the area of the interfacial region. More than 30% of ZEA molecules are distributed in the interfacial region at these temperatures. The question whether these molecules tighten the interfacial region or make this region more permeable still seems to be open and will be addressed in our future experimental and numerical studies.

In conclusion, the model of the DPPC bilayer containing the xanthophyll pigment ZEA is proposed. The experimental data concerning the aggregation of zeaxanthin in DPPC from the literature and from our research were applied as a criterion to fit the model parameters. The model gives the dependences of the main phase transition temperature on ZEA/DPPC molar ratio, the percentage of ZEA in a monomeric form on ZEA/DPPC molar ratio and on temperature. The dependences obtained within the model and the experimental ones are in qualitative agreement. The influence of intermolecular interaction parameters on ZEA aggregation has been discussed. The analyses of the lipid microconfiguration allow formulating the hypothesis concerning the influence of ZEA on the membrane permeability.

## Acknowledgements

This work was supported by a grant from the Medical Academy of Lublin P.W. 564/00 (WO) and by the Maria Curie-Skłodowska University (WG, AS).

## References

- [1] A.J. Young, G. Britton (Eds.), *Carotenoids in Photosynthesis*, Chapman and Hall, London, 1993.
- [2] N.I. Krinsky, The antioxidant and biological properties of the carotenoids, *Ann. NY Acad. Sci.* 854 (1998) 443–447.
- [3] W.I. Gruszecki, Carotenoids in membranes, in: H.A. Frank, A.J. Young, G. Britton, R. Cogdell (Eds.), *The Photochemistry of Carotenoids 8*, Kluwer Academic Publications, Dordrecht, 1999, pp. 363–379.
- [4] K. Strzałka, W.I. Gruszecki, Effect of  $\beta$ -carotene on structural and dynamic properties of model phosphatidylcholine membranes. I. An EPR spin label study, *Biochim. Biophys. Acta* 1068 (1994) 68–72.
- [5] W.K. Subczyński, E. Markowska, J. Siewiewsiuk, Effects of polar carotenoids on the oxygen diffusion-concentration products in lipid bilayers, *Biochim. Biophys. Acta* 1105 (1992) 97–108.
- [6] W.K. Subczyński, E. Markowska, J. Siewiewsiuk, Effect of polar carotenoids on the oxygen diffusion-concentration products in lipid bilayers. An EPR spin label study, *Biochim. Biophys. Acta* 1068 (1991) 68–72.
- [7] W.K. Subczyński, E. Markowska, W.I. Gruszecki, J. Siewiewsiuk, Effect of polar carotenoids on dimyristoylphosphatidylcholine membranes: a spin-label study, *Biochim. Biophys. Acta* 1105 (1992) 97–108.
- [8] A. Wiśniewska, K. Subczyński, Effect of polar carotenoids on the shape of the hydrophobic barrier of phospholipid bilayer, *Biochim. Biophys. Acta* 1368 (1995) 235–246.
- [9] I. Jeżowska, A. Wolak, W.I. Gruszecki, K. Strzałka, Effect of  $\beta$ -carotene on structural and dynamic properties of model phosphatidylcholine membranes. II. A  $^{31}\text{P}$ -NMR and  $^{13}\text{C}$ -NMR study, *Biochim. Biophys. Acta* 1194 (1994) 143–148.
- [10] J. Gabrielska, W.I. Gruszecki, Zeaxanthin (dihydroxy- $\beta$ -carotene) but not  $\beta$ -carotene rigidifies lipid membranes: a  $^1\text{H}$ -NMR study of carotenoid-egg phosphatidylcholine liposomes, *Biochim. Biophys. Acta* 1285 (1996) 167–174.
- [11] V.K. Chaturvedi, C.K.R. Kurup, Interaction of lutein with phosphatidylcholine bilayers, *Biochim. Biophys. Acta* 860 (1986) 286–292.
- [12] V.D. Kolev, D.N. Kafaliev, Miscibility of  $\beta$ -carotene and zeaxanthin with dipalmitoylphosphatidylcholine in multilamellar vesicles: a calorimetric and spectroscopic study, *Photobiophys. Photobiophys.* 11 (1986) 257–267.
- [13] A. Milon, G. Wolf, G. Ourisson, Y. Nakatani, Organization of carotenoid-phospholipid bilayer system. Incorporation of zeaxanthin, astaxanthin and their C50 homologues into dimyristoylphosphatidylcholine vesicles, *Helv. Chim. Acta* 69 (1986) 12–24.
- [14] K. Wójtowicz, W.I. Gruszecki, W. Okulski, A. Juskiewicz, A. Orzechowski, W. Gawda, Phase transition of zeaxanthin modified dimyristoyl phosphatidylcholine liposomes as monitored by acoustic measurements, *Stud. Biophys.* 140 (1991) 115–120.
- [15] K. Wójtowicz, W.I. Gruszecki, Effect of  $\beta$ -carotene, lutein and violaxanthin on structural properties of dipalmitoylphosphatidylcholine liposomes as studied by ultrasound absorption technique, *J. Biol. Phys.* 21 (1995) 73–80.
- [16] A. Gawron, K. Wójtowicz, L.E. Misiak, W.I. Gruszecki, Effects of incorporation of lutein and 8-methoxypsoralen

- into erythrocyte and liposomal membranes, *Pharm. Sci.* 2 (1996) 89–91.
- [17] A. Milon, T. Lazrak, A.M. Albrecht, G. Wolf, G. Weill, G. Ourisson, Y. Nakatani, Osmotic swelling of unilamellar vesicles by the stopped-flow light scattering method. Influence of vesicle size, solute, temperature, cholesterol and three  $\alpha,\omega$ -dihydrocarotenoids, *Biochim. Biophys. Acta* 859 (1986) 1–9.
- [18] T. Lazrak, A. Milon, G. Wolf, A.M. Albrecht, M. Miehé, G. Ourisson, Y. Nakatani, Comparison of the effects of inserted C40- and C50-terminally dihydroxylated carotenoids on the mechanical properties of various phospholipid vesicles, *Biochim. Biophys. Acta* 903 (1987) 132–141.
- [19] C. Socaciu, C. Lausch, H.A. Diehl, Carotenoids in DPPC vesicles: membrane dynamics, *Spectrochim. Acta* 55 (1999) 2289–2297.
- [20] M. Hara, H. Yuan, Q. Yang, T. Hoshino, A. Yokoyama, J. Miyake, Stabilization of liposomal membranes by thermo-zeaxanthins: carotenoid-glucoside esters, *Biochim. Biophys. Acta* 1461 (1999) 147–154.
- [21] L. Cruzeiro-Hansson, O.G. Mouritsen, Passive ion permeability of lipid membranes modelled via lipid-domain interfacial area, *Biochim. Biophys. Acta* 944 (1988) 63–72.
- [22] T. Hønger, K. Jørgensen, R.L. Biltonen, O.G. Mouritsen, Systematic relationship between phospholipase A<sub>2</sub> activity and dynamic lipid bilayer microheterogeneity, *Biochemistry* 28 (1996) 9003–9006.
- [23] T. Brumm, K. Jørgensen, O.G. Mouritsen, T.M. Bayerl, The effect of increasing membrane curvature on the phase transition and mixing behaviour of a dimiristoyl-*sn*-glycero-3-phosphatidylcholine/distearoyl-*sn*-glycero-3-phosphatidylcholine lipid mixture as studied by Fourier transform infrared spectroscopy and differential scanning calorimetry, *Biophys. J.* 70 (1996) 1373–1379.
- [24] D.A. Pink, R. Merkel, B. Quinn, E. Sackmann, J. Pencer, Intersecting polymers in lipid bilayers: cliques, static order parameters and lateral diffusion, *Biochim. Biophys. Acta* 1150 (1993) 189–198.
- [25] M.M. Sperotto, O.G. Mouritsen, Monte Carlo simulation studies of lipid order parameter profiles near integral membrane proteins, *Biophys. J.* 59 (1991) 261–270.
- [26] D.A. Pink, T. Lookman, A.L. MacDonald, M.J. Zuckermann, N. Jan, Lateral diffusion of gramicidin S, M-13 coat protein and glycophorin in bilayers of saturated phospholipids. Mean field and Monte Carlo studies, *Biochim. Biophys. Acta* 687 (1982) 42–56.
- [27] K. Jørgensen, H.J. Ipsen, O.G. Mouritsen, D. Benett, M.J. Zuckermann, A general model for interaction of foreign molecules with lipid membranes: drugs and anaesthetics, *Biochim. Biophys. Acta* 1062 (1991) 227–238.
- [28] O.G. Mouritsen, Computer simulation of cooperative phenomena in lipid membranes, in: R. Brasseur (Ed.), *Molecular Description of Biological Membrane Components by Computer Aided Conformational Analysis*, vol. I, CRC Press, Boca Raton, FL, 1990, pp. 3–83.
- [29] A. Sujak, W. Okulski, W.I. Gruszecki, Organisation of xanthophyll pigments lutein and zeaxanthin in lipid membranes formed with dipalmitoylphosphatidylcholine, *Biochim. Biophys. Acta*, this issue.
- [30] D.A. Pink, T.J. Green, D. Chapman, Raman scattering in bilayers of saturated phosphatidylcholines, *Biochemistry* 19 (1980) 349–356.
- [31] A.M. Ferrenberg, R.H. Swendsen, New Monte Carlo technique for studying phase transitions, *Phys. Rev. Lett.* 61 (1988) 2635–2638.
- [32] C. Huang, Z. Wang, H. Lin, E.E. Brumbaugh, S. Li, Interconversion of bilayer phase transition temperatures between phosphatidylethanolamines and phosphatidylcholines, *Biochim. Biophys. Acta* 1189 (1994) 7–12.
- [33] D. Papahadjopoulos, K. Jacobsen, S. Nir, T. Isac, Phase transitions in phospholipid vesicles. Fluorescence polarisation and permeability measurements concerning the effects of temperature and cholesterol, *Biochim. Biophys. Acta* 311 (1973) 330–348.
- [34] O.G. Mouritsen, K. Jørgensen, H.J. Ipsen, M. Zuckermann, L. Cruzeiro-Hansson, Computer simulation of interfacial fluctuation phenomena, *Phys. Scripta* T33 (1990) 42–51.
- [35] W. Okulski, Distribution of defects in lipid membranes. Computer simulation, *Acta Soc. Bot. Pol.* 3-4 (1996) 257–260.